Modulation of tissue growth heterogeneity by responses to mechanical stress

Antoine Fruleux and Arezki Boudaoud*
Reproduction et Développement des Plantes, Université de Lyon, ENS de Lyon, UCB Lyon 1, INRA, CNRS, 46 Allée d'Italie, 69364 Lyon Cedex 07, France
(Dated: This is A20180906— September 24, 2018)

Morphogenesis often yields organs with robust size and shapes, whereas cell growth and deformation feature significant spatio-temporal variability. Here, we investigate whether tissue responses to mechanical signals contribute to resolve this apparent paradox. We built a model of growing tissues made of fiber-like material, corresponding to the cytoskeleton or the extracellular matrix of animals, or to the cell wall of plants, taking into account the synthesis and remodeling of this fiber-like material, as well as the modulation of synthesis by isotropic and anisotropic response to mechanical stress. Formally, our model describes an expanding, mechanoresponsive, nematic, and active fluid. We show that mechanical responses buffer localized perturbations, with two possible regimes - overdamped relaxation and underdamped relaxation, and the transition between the two corresponds to a minimum value of the relaxation time. Whereas robustness of shapes suggests that growth fluctuations are confined to small scales, our model yields growth fluctuations that have long-range correlations. This indicates that growth fluctuations are a source of heterogeneity in development. Nevertheless, we find that mechanical responses may dampen such fluctuations, with a magnitude of anisotropic response that minimizes heterogeneity of tissue contours. We finally discuss how our predictions might apply to the development of plants and animals. Altogether, our results call for the systematic quantification of fluctuations in growing tissues.

Variability has emerged as an inherent feature of many biological systems (1, 2), spanning molecular scales — such as in cytoskeletal dynamics (3) — to tissular scales — such as in organ expansion (4). For instance, cell growth was found to be spatially heterogeneous (5–9), cell cycle length may appear random (10), and there is extensive evidence of stochastic genetic expression (11, 12). Such variability has been hypothesised to be required for the emergence of complex shapes since it favors symmetry breaking (13) and self-organisation (14) during development. Nevertheless, growth variability would need to be restrained to ensure robust morphogenesis. In plant tissues, an increase in the spatial correlations of growth fluctuations was shown to reduce the robustness of floral organ size and shape (15). In animal tissues, work on the wing imaginal disc of the fruit fly indicates that robust wing development involves cell competition and requires the modulation of cell division and apoptosis (16, 17).

Mechanical signals are natural candidates for the regulation of growth variability because spatial differences in growth or in deformation rates induce mechanical stress (18–20). In animals, a mechanical feedback affecting the rate of cell divisions was hypothesized (21), before being supported by experiments in Drosophila and in zebrafish (22–25). Actomyosin cables are reinforced by mechanical tension in the wing imaginal disk of Drosophila (26). In plants, mechanical sensing was found to be required to prevent growth fluctuations in roots (27). The deposition of cellulose fibers, which are the main load-bearing component of the cell wall, was shown to depend on wall tension (28, 29), which yields cell wall stiffening in the direction of maximal tensile stress (30).

Previous theoretical studies have modelled how mechanical feedback regulates proliferation (21) and how transitions in tissue rheology are induced by proliferation and apoptosis (31, 32) tissues. Here, we build upon such studies; in addition, we account for small sources of stochasticity and investigate the consequences on large scale tissue growth. We focus on generic aspects of tissue growth, so that our results may be broadly applicable to active matter (33).

GROWING TISSUES AS MECHANORESPONSIVE ACTIVE FLUIDS

We built a continuous two-dimensional model of tissue growth. The tissue is assumed to be made of a fiber-like material, which may correspond to the cytoskeleton or to the extra-cellular matrix (ECM) in an animal, and to cellulose within the cell wall of a plant. Hence, the state of the tissue is locally described by two order parameters, the density of fibers and the nematic field describing the orientation of fibers and their degree of alignment, which confer isotropic and anisotropic mechanical properties to the material, respectively. We account for fiber synthesis and remodeling, which may be modulated by responses to mechanical stress: reinforcement of actin stress fibers or of the ECM, enhancement of myosin activity, or fluidisation by cell division, in animals; increase in cell wall synthesis, cellulose synthesis, or cell division, in plants. Synthesis has a small random contribution, considered as a stochastic, uncorrelated source. Stochasticity in synthesis induces growth heterogeneity, which results in mechanical stress and feeds back on synthesis. Formally, the model describes an expanding, mechanoresponsive, nematic, and active fluid.

* Corresponding author: arezki.boudaoud@ens-lyon.fr

A model of nematic viscous fluid

We describe the fibers with a density $\rho(\vec{r})$ and a nematic 2×2 tensor $\overleftrightarrow{s}(\vec{r})$, that vary with the position vector $\vec{r}$. The nematic tensor $\overleftrightarrow{s}$ may be defined as an average over a small region around position $\vec{r}$, $\overleftrightarrow{s}(\vec{r}) = \langle \hat{n}\hat{n} - 1/2\, \overleftrightarrow{1} \rangle_{\vec{r}}$, where the unit vector $\hat{n}$ defines the polarization of fiber monomers and $\overleftrightarrow{1}$ is the unit tensor. Regions of the material move at velocity $\vec{v}(\vec{r})$, which may also vary spatially. In the following, we use the gradient of the velocity field, decomposed into strain rate, $\overleftrightarrow{\gamma} = 1/2 \left\{ (\partial_{\vec{r}} \vec{v}) + (\partial_{\vec{r}} \vec{v})^T \right\}$, and vorticity $\overleftrightarrow{\omega} = 1/2 \left\{ (\partial_{\vec{r}} \vec{v}) - (\partial_{\vec{r}} \vec{v})^T \right\}$, where $\partial_{\vec{r}}$ stands for the partial derivative with respect to position ($\vec{r}$) and ^{T} for the transpose of the preceding tensor.

We neglect diffusion of fibers in the tissue. The equations of continuity for density and nematic tensor are then

$$\partial_t \rho + \partial_{\vec{r}} \cdot \{ \vec{v}\, \rho \} = \kappa_\rho, \qquad [1]$$

$$\partial_t \left\{ \rho \overleftrightarrow{s} \right\} + \partial_{\vec{r}} \cdot \left\{ \vec{v}\, \rho \overleftrightarrow{s} \right\} + \rho \left\{ \overleftrightarrow{\omega} \cdot \overleftrightarrow{s} - \overleftrightarrow{s} \cdot \overleftrightarrow{\omega} \right\} = \overleftrightarrow{\kappa}_s, \quad [2]$$

where t is time, κ_ρ is the rate of synthesis of material, and $\overleftrightarrow{\kappa}_s$ is a nematic tensor that describes the orientation of synthesis and its degree of alignment; the third term of [2] accounts for the corotation of the nematic tensor with flow vorticity.

Expansion of the tissue is assumed to be driven by a uniform and isotropic tension, p, which may correspond to turgor pressure in plants, or to a pressure induced by cell divisions in animals (31); this tension is one of the active components of our model. The mechanical stress, $\overleftrightarrow{\sigma}$, then follows the force balance equation $\partial_{\vec{r}} \cdot \left[\overleftrightarrow{\sigma} - p \overleftrightarrow{1} \right] = \vec{0}$. We consider time scales long enough for tissue remodeling to occur, so that we neglect elastic behavior, assuming that $\overleftrightarrow{\sigma}$ depends on the strain rate tensor, on the density, and on the nematic tensor. This dependence $\overleftrightarrow{\sigma}(\overleftrightarrow{\gamma}, \rho, \overleftrightarrow{s})$ is the constitutive law that characterizes the rheology of the tissue.

In the following, we will consider small fluctuations around an average state. The statistical averages of variables are denoted by brackets. For convenience, tensorial fields $\overleftrightarrow{\Phi} = \Phi \overleftrightarrow{1} + \overleftrightarrow{\Phi}_d$ are decomposed into hydrostatic (Φ) and deviatoric ($\overleftrightarrow{\Phi}_d$) components, $\overleftrightarrow{\Phi}_d$ being traceless. On average, the tissue has uniform density, $\langle \rho \rangle$, and is isotropic, $\langle \overleftrightarrow{s} \rangle = \overleftrightarrow{0}$; the tension $\langle \overleftrightarrow{\sigma} \rangle = \langle \sigma \rangle \overleftrightarrow{1}$ has only a hydrostatic component $\langle \sigma \rangle$; areal growth rate $2\gamma = \partial_{\vec{r}} \cdot v$ is on average uniform; through an appropriate change of reference frame, the averaged velocity may be written as $\langle \vec{v} \rangle = \langle \gamma \rangle \vec{r}$. Assuming small fluctuations in all fields, we linearize the constitutive equation as a function of the hydrostatic strain rate, γ, the deviatoric strain rate, $\overleftrightarrow{\gamma}_d$, the density, ρ, and the nematic tensor $\overleftrightarrow{s}$,

$$\sigma = \langle \sigma \rangle + \eta(1+\nu) \left(\gamma - \langle \gamma \rangle \right) + c_\rho \left(\rho - \langle \rho \rangle \right), \qquad [3]$$

$$\overleftrightarrow{\sigma}_d = \eta(1-\nu) \overleftrightarrow{\gamma}_d + c_s \overleftrightarrow{s}, \qquad [4]$$

where η is an effective viscosity coefficient, c_ρ and c_s are effective compressibilities, and the constant ν is analog to Poisson's ratio.

Activity: mechanical responses and fluctuations

On the one hand, mechanical stress orients cell divisions (22, 23, 34) and plant cell wall reinforcement (30). On the other hand, synthesis of ECM or of cell wall and cytoskeleton polymerization are not uniform in space, having some level of randomness (3, 35, 36). The two classes of phenomena are incorporated in the other active component of our model, namely synthesis. Without loss of generality, synthesis may be written at linear order in fluctuations as

$$\kappa_\rho = \langle \kappa_\rho \rangle - \frac{\langle \rho \rangle}{\tau_\rho} \left(\frac{\rho - \langle \rho \rangle}{\langle \rho \rangle} - \frac{\sigma - \langle \sigma \rangle}{\sigma_\rho} \right) + \xi_\rho, \qquad [5]$$

$$\overleftrightarrow{\kappa}_s = -\frac{\langle \rho \rangle}{\tau_s} \left(\overleftrightarrow{s} - \frac{\overleftrightarrow{\sigma}_d}{\sigma_s} \right) + \overleftrightarrow{\xi}_s, \qquad [6]$$

where τ_ρ and τ_s are the response times of the mechanical feedbacks, σ_ρ and σ_s are constant coefficients determining the amplitudes of the mechanical feedbacks, and ξ_ρ and $\overleftrightarrow{\xi}_s$ are the hydrostatic and deviatoric part of the noise, respectively. Noise is assumed to be white and Gaussian with zero mean, and has extended space correlation characterized by noise strengths $K_{\rho\rho}$ and K_{ss} and by a correlation length ℓ, which is typically sub-cellular or cellular. The correlations functions of noise take the form $\langle \xi_\rho(t_1, \vec{r}_1) \xi_\rho(t_2, \vec{r}_2) \rangle = K_{\rho\rho}\, \delta(t_1 - t_2) g\left(|\vec{r}_1 - \vec{r}_2|/\ell \right)$, and $\langle \overleftrightarrow{\xi}_s(t_1, \vec{r}_1) \overleftrightarrow{\xi}_s(t_2, \vec{r}_2) \rangle = \mathbf{K_{ss}}\, \delta(t_1 - t_2)\, g\left(|\vec{r}_1 - \vec{r}_2|/\ell \right)$. δ is the delta distribution and $g(x)$ is a positive function decaying quickly to zero as $x \to +\infty$. (We use $g(x) = e^{-x}$ in calculations.) Cartesian coordinates of the 4-tensor $\mathbf{K_{ss}}$ are constrained by the traceless nature of $\overleftrightarrow{\xi}_s$ to be of the form $\mathbf{K_{ss}}_{abcd} = K_{ss} \left\{ \delta_{ad}\delta_{bc} + \delta_{ac}\delta_{bd} - \delta_{db}\delta_{cd} \right\}$, where δ_{ij} is the Kronecker delta. We do not take the limit $\ell \to 0$ for spatial correlations because otherwise the problem would have no characteristic lengthscale. Accordingly, we will use ℓ as a unit of length.

Dimensionless parameters

We rescale all fields and variables as follows.

$$\mathsf{P} = c_\rho \frac{\rho - \langle \rho \rangle}{2\eta \langle \gamma \rangle}, \quad \overleftrightarrow{\mathsf{S}} = \frac{c_s}{2\eta \langle \gamma \rangle} \overleftrightarrow{s}, \quad \overleftrightarrow{\Gamma} = \frac{\overleftrightarrow{\gamma} - \langle \overleftrightarrow{\gamma} \rangle}{2\langle \gamma \rangle},$$
$$\Xi_\rho = \frac{c_\rho}{4\eta \langle \gamma \rangle^2} \xi_\rho, \quad \overleftrightarrow{\Xi}_s = \frac{c_s}{4\eta \langle \gamma \rangle^2} \overleftrightarrow{\xi}_s, \quad \overleftrightarrow{\Sigma} = \frac{\overleftrightarrow{\sigma} - \langle \overleftrightarrow{\sigma} \rangle}{2\eta \langle \gamma \rangle},$$
$$\mathsf{T} = 2t \langle \gamma \rangle, \quad \vec{\mathsf{R}} = \frac{\vec{r}}{\ell}, \quad \vec{\mathsf{V}} = \ell \frac{\vec{v} - \langle \vec{v} \rangle}{2\langle \gamma \rangle}.$$

P and $\overleftrightarrow{\mathsf{S}}$ are the dimensionless density fluctuation and nematic tensor. They are associated to the dimensionless random components of synthesis Ξ_ρ and $\overleftrightarrow{\Xi}_s$. $\overleftrightarrow{\Gamma}$ is the dimensionless fluctuation of strain rate tensor, $\overleftrightarrow{\Sigma}$ is the dimensionless stress fluctuation. T, $\vec{\mathsf{R}}$, and $\vec{\mathsf{V}}$ are, respectively, the dimensionless time, position vector, and velocity fluctuation. The dimensionless versions of Eqs. [1-6] are given in **[SI]**.

This rescaling shows that the model has 8 dimensionless parameters. $\omega_\rho = 1 + 1/(2\tau_\rho\langle\gamma\rangle)$ and $\omega_s = 1 + 1/(2\tau_s\langle\gamma\rangle)$ characterize the relaxation of the tissue in absence of mechanical feedback. $\beta_0 = c_\rho\langle\rho\rangle/(2\eta\langle\gamma\rangle)$ characterizes the convexity of growth versus density. ν is the dimensionless difference between effective dilatational and shear viscosities. $\mathsf{K}_{\rho\rho} = K_{\rho\rho}/(16\,\eta^2\langle\gamma\rangle^4)$ and $\mathsf{K}_{ss} = K_{ss}/(16\,\eta^2\langle\gamma\rangle^4)$ are the rescaled magnitudes of random synthesis. $\beta_\rho = c_\rho\langle\rho\rangle/(2\tau_\rho\langle\gamma\rangle\sigma_\rho)$ and $\beta_s = c_s/(2\tau_s\langle\gamma\rangle\sigma_s)$ are the measures of isotropic and anisotropic responses to mechanical stress.

RESPONSE TO PERTURBATIONS IN SYNTHESIS

General results

We consider the tissue size to be much larger than the correlation length, ℓ, and than the characteristic scale of the perturbation. We assume that the perturbations do not induce large scale rotation ($\langle\partial_{\vec{\mathsf{R}}} \wedge \vec{\mathsf{V}}\rangle = \vec{0}$) and we chose the reference frame with origin such that $\vec{\mathsf{V}}(\mathsf{T}, \mathsf{R} = \vec{0}) = \vec{0}$. Given this, we investigate the response to generic perturbations. Because the average strain rate profile stretches all patterns, see [1-2], we consider a modified Fourier transform defined as

$$\widetilde{\Phi}(\vec{q}, \mathsf{T}) = \int d^2\vec{\mathsf{R}}\, e^{-\mathsf{T}}\, e^{-i\vec{q}\cdot\vec{\mathsf{R}}e^{-\mathsf{T}/2}}\Phi(\mathsf{T}, \vec{\mathsf{R}}),$$

with the position $\vec{\mathsf{R}}$ rescaled by the average growth factor $e^{\mathsf{T}/2}$.

Defining $\hat{q} = \vec{q}/|\vec{q}|$ as the direction of the wavevector, the Fourier transform of the nematic tensor can be written as $\overleftrightarrow{\widetilde{\mathsf{S}}} = \widetilde{\mathsf{S}}_{qq}[2\hat{q}\hat{q} - \overleftrightarrow{1}] + \{\hat{q}\,\vec{\vec{\mathsf{S}}}_{q\perp} + \vec{\vec{\mathsf{S}}}_{q\perp}\hat{q}\}$. The linear response for material density and nematic tensor is then given by

$$\begin{bmatrix} \widetilde{\mathsf{P}}(\mathsf{T}, \vec{q}) \\ \widetilde{\mathsf{S}}_{qq}(\mathsf{T}, \vec{q}) \end{bmatrix} = \int_{-\infty}^{\mathsf{T}} d\tau \left[e^{(\tau-\mathsf{T})\,[\omega]} \right] \cdot \begin{bmatrix} \widetilde{\Xi}_\rho(\tau, \vec{q}) \\ \widetilde{\Xi}_{s\,qq}(\tau, \vec{q}) \end{bmatrix},$$

$$\vec{\vec{\mathsf{S}}}_{q\perp}(\mathsf{T}, \vec{q}) = \int_{-\infty}^{\mathsf{T}} d\tau\, e^{\omega_s(\tau-\mathsf{T})}\vec{\vec{\Xi}}_{s\,q\perp}(\tau, \vec{q}),$$

where $\left[e^{(\tau-\mathsf{T})\,[\omega]}\right]$ is a matrix exponential involving the relaxation matrix $[\boldsymbol{\omega}]$, as detailed in **[SI]**, and the fields $\vec{\vec{\Xi}}_{s\,qq} = \hat{q}\cdot\overleftrightarrow{\widetilde{\Xi}}_s(\tau, \vec{q})\cdot\hat{q}$ and $\vec{\vec{\Xi}}_{s\,q\perp} = \hat{q}\cdot\overleftrightarrow{\widetilde{\Xi}}_s(\tau, \vec{q})\cdot[\overleftrightarrow{1} - \hat{q}\hat{q}]$ are the components of the noise Fourier transform.

Finally, the Fourier transform of the strain rate tensor is decomposed as $\overleftrightarrow{\widetilde{\Gamma}} = 2\widetilde{\Gamma}\,\hat{q}\hat{q} + \hat{q}\vec{\widetilde{\Gamma}}_{q\perp} + \vec{\widetilde{\Gamma}}_{q\perp}\hat{q}$, so that the linear response of strain rate is given by,

$$\widetilde{\Gamma}(\mathsf{T}, \vec{q}) = -\int_{-\infty}^{\mathsf{T}} d\tau\, \frac{e^{\omega_\varepsilon(\tau-\mathsf{T})}}{2}\left[C_\rho^\varepsilon\,\widetilde{\Xi}_\rho(\tau, \vec{q}) + C_s^\varepsilon\,\widetilde{\Xi}_{s\,qq}(\tau, \vec{q})\right], \quad [7]$$

$$\vec{\widetilde{\Gamma}}_{q\perp}(\mathsf{T}, \vec{q}) = -\frac{1}{1-\nu}\int_{-\infty}^{\mathsf{T}} d\tau e^{\omega_s(\tau-\mathsf{T})}\,\vec{\vec{\Xi}}_{s\,q\perp}(\tau, \vec{q}), \quad [8]$$

where the integrand in the r.h.s. of [7] is a sum over the values $\{+,-\}$ of the index ε and $\omega_\pm$ are the two eigenvalues of $[\omega]$. The expression of $\omega_\pm$ and the coefficients $C_\varphi^\pm$ can be found in **[SI]**. We thus obtain the full response of the tissue to any perturbation of synthesis, in terms of the modified Fourier transform of the sources of density and of nematic order.

Example: localized disk-shaped isotropic perturbation

As an illustration, we now discuss the case of an isotropic perturbation localised in space – a disk of initial radius ℓ – and in time – a duration that is small with respect to all other time scales. Formally, the perturbation to density synthesis is $\Xi_\rho(\mathsf{T}, \vec{\mathsf{R}}) = \delta(\mathsf{T})\mathrm{H}(1 - |\vec{\mathsf{R}}|)$, with H the Heaviside function, while the perturbation to synthesis of nematic order vanishes, $\overleftrightarrow{\Xi}_s(\mathsf{T}, \vec{\mathsf{R}}) = \overleftrightarrow{0}$. We compute the fields $\Phi = \mathsf{P}, \overleftrightarrow{\mathsf{S}}, \overleftrightarrow{\Sigma}, \overleftrightarrow{\Gamma}$ and find that they have self-similar forms, $\Phi(\mathsf{T}, \vec{\mathsf{R}}) = \mathcal{A}_\Phi(\mathsf{T})\,\mathcal{B}_\Phi(\vec{\mathsf{R}}\,e^{-\mathsf{T}/2})$, where $\mathcal{A}_\Phi$ represents the amplitude of the perturbation and $\mathcal{B}_\Phi$ its pattern. The dynamics of the amplitude is specific to each field, whereas the pattern always expands with a characteristic lengthscale $\ell\exp\langle\gamma\rangle t$ (in dimensional units). $\mathcal{A}_\Phi(T)$ and $\mathcal{B}_\Phi$ are represented in Fig.1**a-e** and are explicitly given in **[SI]**. An immediate consequence of the perturbation is to stiffen the tissue, which reduces expansion ($\mathcal{A}_\Gamma(0) < 0$) and increases stress levels ($\mathcal{A}_\Sigma(0) > 0$); then the anisotropic mechanical response gradually induces radial fibers and reinforcement in the direction of the main stress. The behavior at longer times depends on the levels of mechanical responses. For low anisotropic response, i.e. for β_s smaller than a threshold that depends on other parameters, all amplitudes evolve monotonously as a function of time and vanish at times that are long with respect to the correlation time τ_c; tissue nematic orientation, strain rate, and mechanical stress are all mainly radial. For high anisotropic response, i.e. for β_s above this threshold, amplitudes show an underdamped-like dynamics: they change sign before decaying to 0; after well-defined times, density becomes slightly smaller than average density, and all of nematic

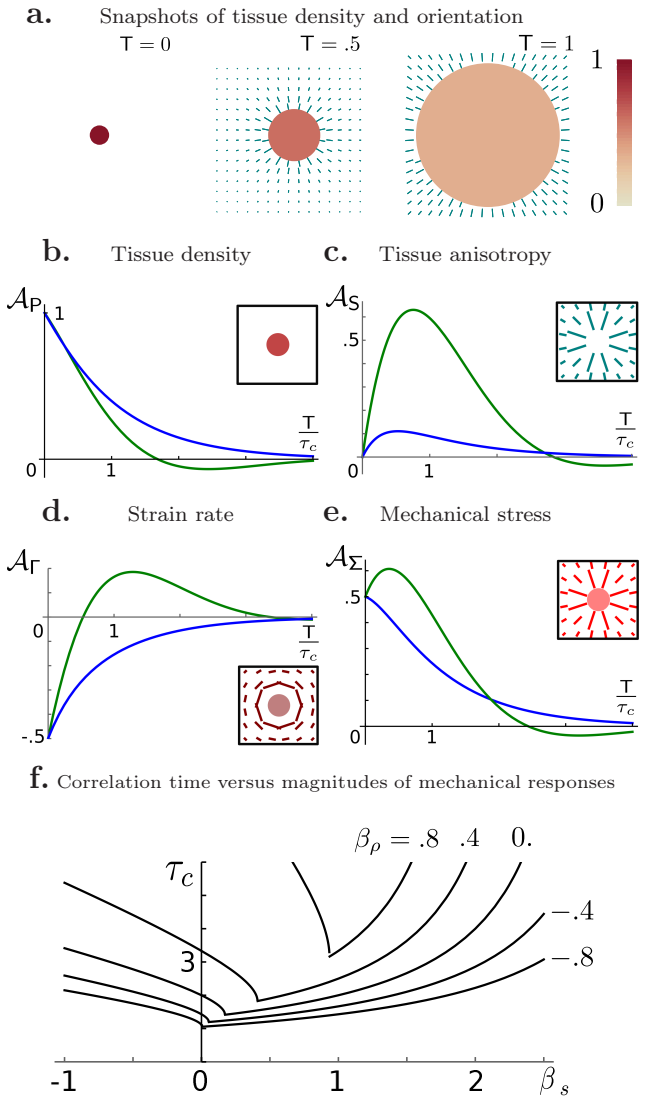

FIG. 1. Example of mechanical response: tissue relaxation following a localized disk-shape isotropic perturbation. **a.** Snapshots at dimensionless times $T = 0$, 0.5 and 1. The density is color-coded according to the heat map on the left (white corresponds to no deviation from average density). The nematic order parameter is shown by the blue lines: the angle corresponds to line orientation and the degree of anisotropy to line length. The mechanical responses strengths are $\beta_s = .3$ and $\beta_\rho = .6$. **b-e** Amplitudes $\mathcal{A}_\varphi$ of the perturbations in tissue density, P, tissue anisotropy, S, strain rate, $\mathsf{\Gamma}$, and mechanical stress, $\mathsf{\Sigma}$; the corresponding patterns ($\mathcal{B}_\varphi$) are shown as insets. The blue and the green lines show the relaxation of the amplitude of the perturbations for low, $\beta_s = 0.3$, and high, $\beta_s = 1.2$, anisotropic response, with $\beta_\rho = .6$. Time is rescaled by the characteristic time, τ_c. **f.** The correlation time, τ_c, as a function of the strength of the isotropic (β_ρ) and anisotropic (β_s) mechanical responses. $\omega_\rho = 1$, $\omega_s = 1$, $\beta_0 = 1$, and $\nu = 0$ for all panels.

order, strain rate, and mechanical stress become circumferential. This underdamped regime can be understood as follows. An initially high mechanical anisotropy of the tissue reduces the radial strain until strain becomes circumferential, leading to circumferential stress and then circumferential nematic order.

These dynamics occur on a time scale τ_c, which is the maximal relaxation time scale in response to a perturbation (see **[SI]**), shown in Fig.1**f** as a function of the magnitudes of mechanical responses. Isotropic mechanical feedback makes perturbations more persistent, because τ_c increases with β_ρ. The effect of the anisotropic feedback on relaxation is more complex: τ_c first decrease and then increase as β_s is increased; the minimum of τ_c corresponds to the transition between the overdamped and the underdamped regimes. This characteristic time τ_c will also appear to be important for the effect of noise.

GROWTH FLUCTUATIONS

Correlation functions

Using the linear response of flow velocity to synthesis perturbations [7-8], we derived the velocity fluctuations, as detailed in **[SI]**. The correlation tensor of velocity fluctuations is proportional to the unit tensor,

$$\langle \vec{\mathsf{V}}(\mathsf{T},\vec{\mathsf{R}}_1)\vec{\mathsf{V}}(\mathsf{T}+\Delta\mathsf{T},\vec{\mathsf{R}}_2)\rangle = \overset{\leftrightarrow}{1}\Big\{\mathsf{K}_{\varphi_1\varphi_2}C^{\varepsilon_1}_{\varphi_1}C^{\varepsilon_2}_{\varphi_2}\mathcal{I}(\vec{\mathsf{R}}_1,\vec{\mathsf{R}}_2,\Delta\mathsf{T},\omega_{\varepsilon_1},\omega_{\varepsilon_2}) + 4\mathsf{K}_{ss}/(1-\nu)^2\,\mathcal{I}(\vec{\mathsf{R}}_1,\vec{\mathsf{R}}_2,\Delta\mathsf{T},\omega_s,\omega_s)\Big\}, \quad [9]$$

for $\Delta\mathsf{T} > 0$, with the same $C^{\pm}_{\varphi}$ coefficients as in [7-8] and

$$\mathcal{I}(\vec{\mathsf{R}}_1,\vec{\mathsf{R}}_2,\Delta\mathsf{T},\omega_1,\omega_2) = e^{\Delta\mathsf{T}(\frac{1}{2}-\omega_1)}\Big\{I(|\vec{\mathsf{R}}_2|e^{-\frac{\Delta\mathsf{T}}{2}},\omega_1+\omega_2) + I(|\vec{\mathsf{R}}_1|,\omega_1+\omega_2) - I(|\vec{\mathsf{R}}_1-\vec{\mathsf{R}}_2e^{-\frac{\Delta\mathsf{T}}{2}}|,\omega_1+\omega_2)\Big\},$$

where $I(\mathsf{R},\omega) = \frac{1}{2}\int_{-\infty}^{0} d\tau e^{\tau(\omega-1)}\int_0^{\mathsf{R}\,e^{\tau/2}}\frac{dx}{x}\int_0^x dr\,r\,g(r)$. This explicitly defines the correlation functions, which we analyse in the following section. In particular, the correlation function of the areal strain rate has power-law tails, $\langle\mathsf{\Gamma}(\vec{\mathsf{R}}_1)\mathsf{\Gamma}(\vec{\mathsf{R}}_2)\rangle \sim \|\vec{\mathsf{R}}_1-\vec{\mathsf{R}}_2\|^{-\alpha}$, yielding long-range correlations.

Results

In practice, growth (areal strain rate in 2D) is measured at the scale of the spatial resolution of experiments, which may be the cell scale or larger scales depending on the landmarks used. We therefore define a coarse-grained growth rate and we consider the time correlation function $G(\mathsf{R},\mathsf{T})$ of the growth of a disk of radius R, where R is the coarse-graining size i.e. the resolution size. It is simply related to velocity fluctuations by $G(\mathsf{R},\mathsf{T}) = 1/(\pi\,\mathsf{R}^2)^2\langle\int_0^{2\pi}d\theta\int_0^{2\pi}d\varphi\,\vec{\mathsf{R}}(\theta)\cdot\vec{\mathsf{V}}(\vec{\mathsf{R}}(\theta),0)\;\vec{\mathsf{R}}(\varphi)\cdot\vec{\mathsf{V}}(\vec{\mathsf{R}}(\varphi),\mathsf{T})\rangle$. This correlation function

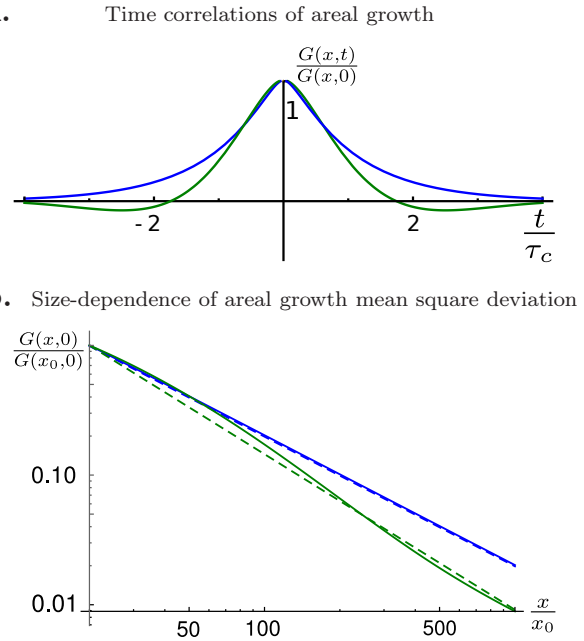

FIG. 2. Growth fluctuations. **a.** Time correlation function $G(\mathsf{R},\mathsf{T})$ (normalized by its initial value) as a function of time, T, normalized by the correlation time, τ_c. The blue and green curves correspond to low ($\beta_s = .3$) and high ($\beta_s = 1.2$) anisotropic mechanical response, with $\beta_\rho = .6$. **b.** Growth mean square deviation, $G(\mathsf{R},\mathsf{T})$, as a function of the coarse-graining size, R, for low (blue) and high (green) anisotropic mechanical response. $G(\mathsf{R},\mathsf{T})$ and R are normalized using $\mathsf{R}_0 = 10$. The asymptotic power-law for low anisotropic mechanical response is shown by the blue dashed line. For high anisotropic mechanical response, $G(\mathsf{R},\mathsf{T})$ oscillates around a power-law (dashed green line). $\omega_\rho = 1$, $\omega_s = 1$, $\beta_0 = 1$, and $\nu = 0$ for the two panels.

is plotted in Fig.2. Panel **a** shows time correlations for high and low anisotropic mechanical feedback, respectively corresponding to the overdamped and the underdamped regimes. The negative correlations for high feedback are related to underdamped relaxation. The correlation function decays quickly to 0 with a characteristic time scale that is exactly the relaxation time, τ_c, shown in Fig.2**e**. Areal growth mean square deviation appears roughly scale-invariant, see Fig.2**b**; it is exactly scale-invariant in the overdamped regime and oscillates around a scale-invariant trend in the underdamped regime. Two regimes are observed, that are unrelated to the overdamped and underdamped regimes already described. When $\tau_c < 2$, growth mean square deviation scales with the inverse of the coarse-graining area, $G(\mathsf{R},0) \sim \mathsf{R}^{-2}$, an exponent due to the central limit theorem. When $\tau_c > 2$, growth mean square deviation decays more slowly with the coarse-graining area, $G(\mathsf{R},0) \sim \mathsf{R}^{-4/\tau_c}$, see **[SI]** for a rationale.

FLUCTUATIONS OF ORGAN SHAPE

We are now interested in the effects of noise in synthesis on tissue contours or on organ shape. In a homogeneous and isotropic tissue, quantifying the fluctuation of contours is equivalent to determining the fluctuation of a vector joining two landmarks followed throughout growth of the tissue. Hence, we use a Lagrangian description and consider the position, $\vec{X}(\mathsf{T})$, at time T of a landmark initially at position $\vec{X}_0$, which is determined by the dimensionless velocity field $\vec{\mathsf{V}}$ through

$$\frac{d\vec{X}(\mathsf{T})}{d\mathsf{T}} = \frac{1}{2}\vec{X}(\mathsf{T}) + \vec{\mathsf{V}}(\mathsf{T}, \vec{X}(\mathsf{T})).$$

In the following, we compute the fluctuations of $\vec{X}$.

Formulation

We look for the probability $\mathcal{P}\left[\vec{X}(\mathsf{T})\right]$ that a material point follows a path $\vec{X}(\mathsf{T})$. For sufficiently small fluctuations, this probability can be explicitly derived from the statistical properties of $\vec{\mathsf{V}}$ and simplified as

$$\mathcal{P}\left[\vec{X}(\mathsf{T})\right] \sim \delta(\vec{X}(0) - \vec{X}_0)\, e^{-\mathcal{A}\left[\vec{X}(\mathsf{T})\right]}, \qquad [10]$$

$$\mathcal{A}\left[\vec{X}(\mathsf{T})\right] = \int d\mathsf{T} \frac{\left|\frac{\vec{X}(\mathsf{T})}{d\mathsf{T}} - \frac{1}{2}\vec{X}(\mathsf{T})\right|^2}{2\int_0^\infty d\tau e^{-\frac{\tau}{2}} \langle \vec{\mathsf{V}}(0, \vec{X}(\mathsf{T})) \cdot \vec{\mathsf{V}}(\tau, \vec{X}(\mathsf{T}) e^{\frac{\tau}{2}}) \rangle},$$

where the correlation function $\langle \vec{\mathsf{V}}(\vec{X}_1, \mathsf{T}_1)\vec{\mathsf{V}}(\vec{X}_2, \mathsf{T}_2)\rangle$ is given by [9]. We determined the asymptotic statistics of the Lagrangian flow by applying the saddle point method (37) to the probability $\mathcal{P}$. As expected, $\mathcal{P}$ is maximized by the average trajectory $\langle \vec{X}(\mathsf{T})\rangle = \vec{X}_0\, e^{\mathsf{T}/2}$. The correlation tensor of the position $\vec{X}(\mathsf{T})$ is given by (see **[SI]**, for details)

$$\langle \Delta\vec{X}(\mathsf{T}_1)\Delta\vec{X}(\mathsf{T}_2)\rangle = \qquad [11]$$
$$\overset{\leftrightarrow}{1}\, X_0^2 e^{\frac{\mathsf{T}_2+\mathsf{T}_1}{2}} \mathcal{J}\left(X_0 e^{\frac{\mathsf{T}_2}{2}}\right)\left(1 - \mathcal{J}\left(X_0 e^{\frac{\mathsf{T}_1}{2}}\right)/\mathcal{J}\left(X_0\right)\right),$$

$$\mathcal{J}(u) = \frac{1}{u^2}\int_0^\infty dt' \int_0^\infty d\tau \langle \vec{\mathsf{V}}(0, u\, e^{\frac{t'}{2}}) \cdot \vec{\mathsf{V}}(\tau, u\, e^{\frac{t'+\tau}{2}})\rangle e^{-t'-\frac{\tau}{2}},$$

with $\mathsf{T}_1 \leq \mathsf{T}_2$ and $X_0 = \|\vec{X}_0\|$. Note that this correlation tensor is not a function of $\mathsf{T}_2 - \mathsf{T}_1$ because of the lack of invariance with respect to translations in time.

Results

Heterogeneity in development can be quantified by the coefficient of variation, $\mathrm{CV}(\mathsf{T}) =$

$\langle\|\Delta\vec{X}(\mathsf{T})\|^2\rangle^{1/2}/\langle\|\vec{X}(\mathsf{T})\|\rangle$, which is plotted in Fig.3**a**. Its asymptotic trend for long times depends on the value of the correlation time τ_c. If $\tau_c < 2$, then CV $\sim \mathsf{T}^{1/2}e^{-\mathsf{T}}$, and for $\tau_c > 2$, CV scales $e^{-2\mathsf{T}/\tau_c}$ for low feedback and oscillate around this trend for high feedback.

We represent in Fig.3**b** the maximal value of the coefficient of variation, normalized by $\mathsf{K}_{\rho\rho}^{1/2}$. This enables us to assess the fluctuations of contours in the tissue or of organ shapes. In absence of anisotropic feedback, $\beta_s = 0$, we find that heterogeneity increases with as isotropic feedback. Accordingly, a positive isotropic feedback maintains perturbations and induces long-range correlations as seen in previous sections. Conversely, negative isotropic feedback dampens perturbations. In absence of isotropic feedback, $\beta_\rho = 0$, we find that heterogeneity has a single minimum, decreasing with anisotropic feedback below this minimum, and increasing above. The transition at the minimum corresponds to the transition between the overdamped and the underdamped regime. In the overdamped regime, increasing anisotropic feedback dampens perturbations. In the overdamped regime, increasing anisotropic feedback enhances perturbations due to the oscillatory overshoot. In general, for $\beta_\rho \neq 0$ and $\beta_s \neq 0$, the two trends previously described are combined. Finally, we note that the behavior of heterogeneity in Fig.3**b** is qualitatively similar to the behavior of correlation time (τ_c) in Fig.1**f**, indicating that the correlation time is a major factor for the level of heterogeneity because the correlation time sets how the tissue keeps a memory of its previous state.

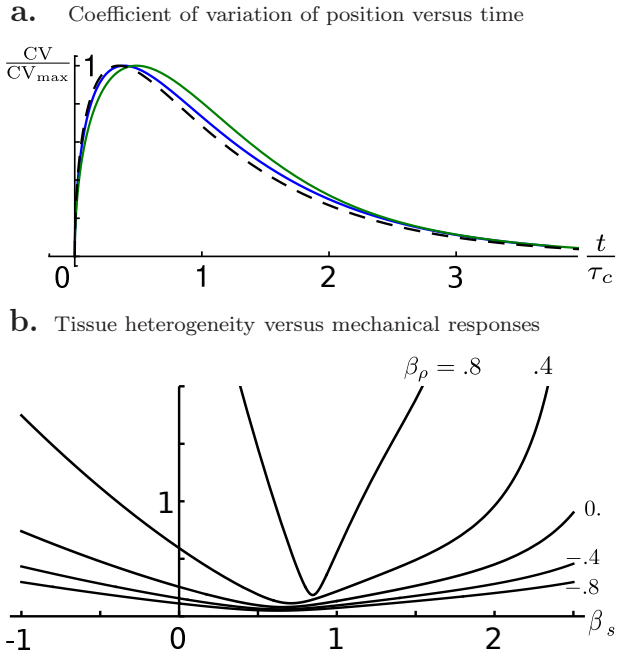

FIG. 3. **a.** Coefficient of variation of position, $\langle\|\Delta\vec{X}(\mathsf{T})\|^2\rangle^{1/2}/\langle\|\vec{X}(\mathsf{T})\|\rangle$, normalized by its maximal value $\mathrm{CV}_{\max}$ as a function of time, T, normalized by the correlation time, τ_c.The blue and the green curve are examples of low $\beta_s = .3$ and high $\beta_s = 1.2$ anisotropic mechanical response, with $\beta_\rho = .6$. The dashed line represents the asymptotic limit for $X_0 \gg 1$ for low anisotropic feedback. **b.** Coefficient of variation of position, normalized by $\mathsf{K}_{\rho\rho}^{1/2}$, as a function of the magnitude of anisotropic mechanical response for various levels of anisotropic feedback. $\omega_\rho = 1$, $\omega_s = 1$, $\beta_0 = 1$, $\nu = 0$, and $X_0 = 10$ for the two panels.

DISCUSSION

We built a continuous model of tissue growth, describing density and nematic order of the tissue, and modelled material synthesis and responses to mechanical stress. The responses are characterized by two parameters, β_ρ and β_s, corresponding to isotropic response - increase in density due to increase in stress when $\beta_\rho > 0$ - and anisotropic response - increase in tissue anisotropy due to increase in stress anisotropy when $\beta_s > 0$, and conversely when these parameters are negative. In plants, it is believed that cell wall synthesis is enhanced when tension increases (38), which corresponds to $\beta_\rho > 0$. The alignment of cortical microtubules with maximal stress orientation leads to the anisotropic stiffening of the cell wall in this direction (30, 39), while cell divisions are associated with new cell walls oriented in the direction of maximal stress (34); both processes yield $\beta_s > 0$. In animal tissues, experiments indicate that tissues are fluidised by cell divisions (22–25): proliferation is enhanced by tensile stress and daughter cells tend to separate along the direction of highest mechanical stress, which corresponds to $\beta_\rho < 0$ and $\beta_s < 0$, respectively. At shorter time scales, actomyosin cables are reinforced in the direction of applied stress (26), which yields $\beta_\rho > 0$. It is unclear how ECM remodeling would contribute to mechanical responses, because its role in morphogenesis has not received attention until recently (40–43).

In this study, we determined tissue response to a localized perturbation, as a function of the mechanical feedback parameters β_ρ and β_s. We generalized predictions that anisotropic mechanical feedback buffers such a perturbation (29), in agreement with observations on trichomes, a cell type with transient faster growth, in Arabidopsis sepals (29). Here, we unravelled two possible regimes: an overdamped regime at low anisotropic feedback in which perturbations decay monotonously and an underdamped regime at high anisotropic feedback in which perturbations oscillate before decaying, with a characteristic time that is minimal at the transition between the two regimes. This case study provides an assay of mechanical responses in both plant and animal systems, for instance by inducing clones with altered growth rate and quantifying the relaxation timescales in backgrounds with different levels of mechanical response.

We then investigated the statistical properties of tissue growth, unravelling long-range correlations, with slowly decaying correlation functions. To test this, it would crucial to examine correlation functions in live imaging data of growing organs, e.g. (15, 44–47). Long-range correla-

tions could be mediated by signals that could be chemical or mechanical. Further experiments would be required to test whether mechanical signals are involved in such correlations.

Finally, we found that heterogeneity of contours and shapes is minimal for a well-determined level of anisotropic mechanical response. This generalizes a similar conclusion reached for local heterogeneity using a cell-based toy model (48). Here we also accounted for isotropic mechanical responses and considered heterogeneity at all scales. We identified the correlation time as a key parameter determining the extent of spatial correlations and the level of heterogeneity of organ shape. Based on our results, we make the following predictions. In plants ($\beta_\rho > 0$ and $\beta_s > 0$), heterogeneity in development can be significantly high unless anisotropic feedback is close to the value that minimizes heterogeneity. In animals, if we discard possible contributions of the ECM, $\beta_\rho < 0$ and $\beta_s < 0$ at long time scales, heterogeneity in development is minimal when anisotropic feedback is negligible. Based on our results, we propose that the robustness of morphogenesis constrains how tissues respond to mechanical stress. More generally, characterizing the fluctuations of cell properties appears as a promising avenue to shed light on how signals orchestrate organismal development.

[1] H. M. Meyer and A. H. Roeder, Frontiers in plant science **5**, 420 (2014).
[2] A. C. Oates, Development **138**, 601 (2011).
[3] D. S. Banerjee, A. Munjal, T. Lecuit, and M. Rao, Nature Communications **8**, 1121 (2017).
[4] M. Sahaf and E. Sharon, Journal of experimental botany **67**, 5509 (2016).
[5] M. Uyttewaal, A. Burian, K. Alim, B. Landrein, D. Borowska-Wykręt, A. Dedieu, A. Peaucelle, M. Ludynia, J. Traas, A. Boudaoud, et al., Cell **149**, 439 (2012).
[6] G. Tauriello, H. M. Meyer, R. S. Smith, P. Koumoutsakos, and A. H. Roeder, Plant physiology **169**, 2342 (2015).
[7] D. Kierzkowski, N. Nakayama, A.-L. Routier-Kierzkowska, A. Weber, E. Bayer, M. Schorderet, D. Reinhardt, C. Kuhlemeier, and R. S. Smith, Science **335**, 1096 (2012).
[8] J. Elsner, M. Michalski, and D. Kwiatkowska, Annals of botany **109**, 897 (2012).
[9] S. L. Martin, Nature **460**, 1087 (2009).
[10] A. H. Roeder, V. Chickarmane, A. Cunha, B. Obara, B. Manjunath, and E. M. Meyerowitz, PLoS biology **8**, e1000367 (2010).
[11] A. Raj and A. van Oudenaarden, Cell **135**, 216 (2008).
[12] I. S. Araújo, J. M. Pietsch, E. M. Keizer, B. Greese, R. Balkunde, C. Fleck, and M. Hülskamp, Nature communications **8**, 2132 (2017).
[13] F. Corson, L. Couturier, H. Rouault, K. Mazouni, and F. Schweisguth, Science **356**, eaai7407 (2017).
[14] J. R. Chubb, Wiley Interdisciplinary Reviews: Developmental Biology **6** (2017).
[15] L. Hong, M. Dumond, S. Tsugawa, A. Sapala, A.-L. Routier-Kierzkowska, Y. Zhou, C. Chen, A. Kiss, M. Zhu, O. Hamant, et al., Developmental cell **38**, 15 (2016).
[16] D. R. Hipfner and S. M. Cohen, Nature Reviews Molecular Cell Biology **5**, 805 (2004).
[17] M. Milán, S. Campuzano, and A. García-Bellido, Proceedings of the National Academy of Sciences **93**, 640 (1996).
[18] K. D. Irvine and B. I. Shraiman, Development **144**, 4238 (2017).
[19] V. Mirabet, P. Das, A. Boudaoud, and O. Hamant, Annual review of plant biology **62**, 365 (2011).
[20] G.-J. J. Gao, M. C. Holcomb, J. H. Thomas, and J. Blawzdziewicz, Journal of Physics: Condensed Matter **28**, 414021 (2016).
[21] B. I. Shraiman, Proceedings of the National Academy of Sciences of the United States of America **102**, 3318 (2005).
[22] L. LeGoff, H. Rouault, and T. Lecuit, Development **140**, 4051 (2013).
[23] P. Campinho, M. Behrndt, J. Ranft, T. Risler, N. Minc, and C.-P. Heisenberg, Nature cell biology **15**, 1405 (2013).
[24] Y. Mao, A. L. Tournier, A. Hoppe, L. Kester, B. J. Thompson, and N. Tapon, The EMBO journal **32**, 2790 (2013).
[25] Y. Pan, I. Heemskerk, C. Ibar, B. I. Shraiman, and K. D. Irvine, Proceedings of the National Academy of Sciences **113**, E6974 (2016).
[26] M. Duda, N. Khalilgharibi, N. Carpi, A. Bove, M. Piel, G. Charras, B. Baum, and Y. Mao, bioRxiv , 241497 (2017).
[27] H.-W. Shih, N. D. Miller, C. Dai, E. P. Spalding, and G. B. Monshausen, Current Biology **24**, 1887 (2014).
[28] O. Hamant, M. G. Heisler, H. Jönsson, P. Krupinski, M. Uyttewaal, P. Bokov, F. Corson, P. Sahlin, A. Boudaoud, E. M. Meyerowitz, et al., science **322**, 1650 (2008).
[29] N. Hervieux, S. Tsugawa, A. Fruleux, M. Dumond, A.-L. Routier-Kierzkowska, T. Komatsuzaki, A. Boudaoud, J. C. Larkin, R. S. Smith, C.-B. Li, et al., Current Biology **27**, 3468 (2017).
[30] A. Sampathkumar, P. Krupinski, R. Wightman, P. Milani, A. Berquand, A. Boudaoud, O. Hamant, H. Jönsson, and E. M. Meyerowitz, eLife **3**, e01967 (2014).
[31] J. Ranft, M. Basan, J. Elgeti, J.-F. Joanny, J. Prost, and F. Jülicher, Proceedings of the National Academy of Sciences **107**, 20863 (2010).
[32] D. Matoz-Fernandez, E. Agoritsas, J.-L. Barrat, E. Bertin, and K. Martens, Physical review letters **118**, 158105 (2017).
[33] M. C. Marchetti, J.-F. Joanny, S. Ramaswamy, T. B. Liverpool, J. Prost, M. Rao, and R. A. Simha, Reviews of Modern Physics **85**, 1143 (2013).
[34] M. Louveaux, J.-D. Julien, V. Mirabet, A. Boudaoud, and O. Hamant, Proceedings of the National Academy of Sciences **113**, E4294 (2016).
[35] B. Altartouri and A. Geitmann, Current opinion in plant biology **23**, 76 (2015).

[36] C. T. Anderson, I. S. Wallace, and C. R. Somerville, Proceedings of the National Academy of Sciences **109**, 1329 (2012).
[37] A. Altland and B. D. Simons, Condensed matter field theory (Cambridge University Press, 2010) Chap. 3, pp. 108–111.
[38] S. Wolf, K. Hématy, and H. Höfte, Annual review of plant biology **63**, 381 (2012).
[39] B. Landrein and O. Hamant, The Plant Journal **75**, 324 (2013).
[40] J. Crest, A. Diz-Muñoz, D.-Y. Chen, D. A. Fletcher, and D. Bilder, Elife **6**, e24958 (2017).
[41] R. P. Ray, P. S. Ganguly, S. Alt, J. R. Davis, A. Hoppe, N. Tapon, G. Salbreux, B. J. Thompson, et al., Developmental cell **46**, 23 (2018).
[42] J. Chlasta, P. Milani, G. Runel, J.-L. Duteyrat, L. Arias, L.-A. Lamiré, A. Boudaoud, and M. Grammont, Development , dev (2017).
[43] R. Loganathan, B. J. Rongish, C. M. Smith, M. B. Filla, A. Czirok, B. Bénazéraf, and C. D. Little, Development **143**, 2056 (2016).
[44] I. Heemskerk, T. Lecuit, and L. LeGoff, Development **141**, 2339 (2014).
[45] B. Guirao, S. U. Rigaud, F. Bosveld, A. Bailles, J. López-Gay, S. Ishihara, K. Sugimura, F. Graner, and Y. Bellaïche, Elife **4**, e08519 (2015).
[46] E. Rozbicki, M. Chuai, A. I. Karjalainen, F. Song, H. M. Sang, R. Martin, H.-J. Knölker, M. P. MacDonald, and C. J. Weijer, Nature cell biology **17**, 397 (2015).
[47] E. E. Kuchen, S. Fox, P. B. De Reuille, R. Kennaway, S. Bensmihen, J. Avondo, G. M. Calder, P. Southam, S. Robinson, A. Bangham, et al., Science **335**, 1092 (2012).
[48] K. Alim, Frontiers in Plant Science **3**, 1 (2012).